bFGF Up-regulation Reduces Spontaneous Necrosis of VX2 Tumors Without Increasing Tumoral Microvascular Density

FLORENTINA PASCALE[1], SAIDA-HOMAYRA GHEGEDIBAN[1,3], LAURENT BEDOUET[1], JULIEN NAMUR[1], MICHEL BONNEAU[2], VALENTIN VERRET[1], ISABELLE SCHWARTZ-CORNIL[5], MICHEL WASSEF[3,4] and ALEX LAURENT[2,4,6]

[1]ArchimMed, Jouy en Josas, France;
[2]Research Center for Interventional Imaging, National Institute of Agronomic Research, Jouy-en-Josas, France/Public Assistance & Paris Hospitals, Paris, France;
Departments of [3]Pathology, and 6Interventional Neuroradiology, Lariboisière Hospital, Public Assistance & Paris Hospitals, Paris, France;
[4]Faculty of Medicine, Diderot University Paris, Paris, France;
[5]Laboratory of Virology and Molecular Immunology, National Institute of Agronomic Research, Jouy en Josas, France

Abstract. *Aim: To determine whether up-regulation of basic fibroblast growth factor (bFGF) in VX2 cells reduces tumor necrosis. Materials and Methods: VX2 cells were transfected with expression vector containing cDNA of rabbit bFGF. Stable clones producing rabbit bFGF (bFGF-VX2) were selected. bFGF-VX2 (n=5) or non-transfected VX2 (control) (n=5) cells were implanted into leg muscle of 10 rabbits. The tumors were characterized 21 days after grafting. Results: Overexpression of bFGF by VX2 tumors significantly reduced necrosis ($p<0.0223$) and increased cell viability ($p<0.0223$), without effect on the mean vascular density. bFGF concentration was significantly higher in bFGF-VX2 tumors ($p<0.0062$) and negatively correlated with tumor volume at day 21 ($\varrho=-0.927$, $p<0.0034$). Vascular endothelial growth factor concentration was significantly lower in bFGF-VX2 tumors ($p<0.0105$) and negatively correlated with the bFGF concentration of tumors ($\varrho=-0.903$, $p<0.0067$). Conclusion: The overexpression of bFGF in VX2 cells increased tumor viability and reduced necrosis, making the evaluation of long-term anticancer therapies possible in this model.*

Correspondence to: Florentina Pascale, Archimmed SARL, 12 rue Charles de Gaulle, 78350, Jouy en Josas, France. Tel: +33 683913439, Fax: +33 139200710, e-mail: florentina.pascale@archimmed.com

Key Words: VX2, VEGF, bFGF, transfection, plasmid, clones, experimental tumors, necrosis, vessel density, rabbit, animal models.

The VX2 tumor is a carcinoma serially transplantable in allogenic adult rabbits, easily implantable, which grows quickly in many organs (1, 2). VX2 has been extensively used for the evaluation of the efficacy of locoregional therapies, mainly transcatheter arterial chemoembolisation, thanks to its similarities with localized hepatoma (3).

However, despite its ability to grow in many organs, VX2 carcinoma has its limitations because of its high rate of spontaneous necrosis (2, 4). This especially limits the application of this model for the long-term evaluation of necrosis induced by chemo- or radiotherapeutic locoregional therapies or *in situ* ablation therapies.

A strategy to improve tumor angiogenesis can be based on the manipulation of the two most important factors involved in tumor angiogenesis, namely vascular endothelial growth factor (VEGF) and basic fibroblast growth factor (bFGF). Transfection of VX2 tumor cells with a VEGF-encoding vector increased the tumor volume, the mean vascular density (MVD) and reduced tumor necrosis by two-fold (5). Overexpression of bFGF in many tumor cells accelerates tumor progression, increases the MVD and inhibits apoptosis (6-9).

The objective of the present study was to set up a reproducible VX2 tumoral model with a stable level of bFGF secretion, well-defined angiogenic phenotype and reduced necrosis.

With this aim, a VX2 cell line was transfected with bFGF-encoding vector to obtain clones with controlled expression levels of bFGF. These modified cells were then implanted into New Zealand White rabbits in order to examine the grafting, growth, vascularization and necrosis of tumors.

Materials and Methods

Transfection of VX2 cells with bFGF-encoding vectors. The vector containing bFGF sequence was constructed by cloning the cDNA of rabbit bFGF (http://www.ensembl.org) in a eukaryotic expression vector Gateway® pDEST™ 26 Vector (Invitrogen Life Technologies SAS, Saint Aubin, France) under control of cytomegalovirus gene promoter (Gene Art, Regensburg, Germany).

VX2 cell line isolated and cultured as previously described (5) was transfected with rabbit bFGF. Cells were plated (5×10^4 cells/ml) and transfected with the vector containing rabbit bFGF cDNA, using Lipofectamine 2000 transfection kit (Invitrogen Life Technologies SAS, Saint Aubin, France), following the manufacturer's instructions. At 48 h later, cells were passaged in medium containing the G418 antibiotic at 1 mg/ml (Sigma, Saint Louis, MO, USA). The medium was changed every 48-72 h over 14 days until G418-resistant clones were observed. The most isolated colonies were cloned and transferred to a 96-well culture plate.

For bFGF detection in cell-culture supernatants, the cells were seeded at 1×10^5 in 2 ml medium in a culture dish for 72 h. The conditioned medium was then collected and the cells trypsinized and counted (to normalize data). bFGF concentrations were measured by mean of enzyme-linked immunosorbent assay (ELISA) (Human bFGF ELISA; RayBio Inc., Norcross, Canada). A clone with the highest *in vitro* level of bFGF production (bFGF-VX2) was selected for implantations.

Animal implantation. The experimental procedures were performed at the Center of Research in Interventional Radiology (Cr2i/APHP/National Institute of Agronomic Research INRA; Jouy en Josas, France). All experiments were approved by the Institutional Animal Care and Use Committee of the Center and were conducted according to European Community rules of animal care (Directive EC 86/609) number 08-008.

Ten adult New Zealand White rabbits (Unité Commune d'Experimentation Animale, National Institute of Agronomic Research, Jouy-en-Josas, France) were implanted with bFGF-VX2 cells (n=5) or with VX2 non-transfected cells for controls, (n=5). Short 'flash' mask anesthesia was performed with 5% isoflurane (Aerrane, Baxter, France) and 95% O_2 for 5 min then 10^8 cells in 0.5 ml RPMI were slowly injected into the leg muscle of the anesthetized rabbits.

Tumor growth. Tumor growth was monitored *in vivo* by ultrasound, at day 10, 13 and 17, using a 5-mHz abdominal transducer (Voluson E8 Expert; GE Healthcare, Velizy, France). The tumor volume was calculated by the formula: $\pi/6$ (abc), where a, b and c were the length, width and thickness of the tumor as described previously (5). Animals were sacrificed on day 21 after implantation by intravenous injection of pentobarbital (5 ml, 200 mg/ml; Doléthal, Vétoquinol, France). The tumors were harvested and their length, width and thickness were measured with a caliper. Their volume was then calculated as described above.

Histology. The histological aspect of the tumors was analyzed by an experimented pathologist. After formalin fixation for at least 48 h, and paraffin-embedding, two axial slices (5 μm-thick) representing the most central part of the tumor were stained with hematoxylin-eosin-saffron (HES). Two axial slides were stained with red Sirius for connective tissue quantification. Two axial slides were stained with antibodies to cytokeratin 3 for quantification of viable tumoral tissue as described below. Each slide stained with HES, red Sirius and cytokeratin 3 were examined under light microscopy (Leitz Diaplan, Leitz, France) and sections were digitized with Cartograph software (Microvision Instruments, Paris, France), using an Axoplan microscope (Zeiss, Le Pecq, France) with a motorized plate and a video camera. Digital images were imported into ImageJ software (Image J, 1.42 q; National Institutes of Health, Bethesda, MD, USA). Necrosis, cysts, connective tissue and viable tumoral tissue extent were quantified by grid method (5) and expressed as a percentage of the entire tumor area. Cystic cavities were quantified as the empty area in the tumor body surrounded by a flattened layer of tumor cells.

Immunohistochemistry. Two consecutive slides were stained with anti-cytokeratin 3 antibodies (mouse anti-human cytokeratin clones AE1-AE3; Dako Glostrup, Denmark) at 1/50 dilution for tumoral cell staining or with monoclonal antibodies to CD31 (JC70A; Dako) diluted at 1/20 for 30 min for vessel staining, and then with a horse anti-mouse secondary antibody (Vector Laboratories, Burlingame, CA, USA) for 30 min at room temperature, and the reaction was revealed by 3-3'-diaminobenzidine tetrahydrochloride substrate.

Vessel density was evaluated by counting the CD31-stained vessels on two tumor slices as described elsewhere (5). The tumor sections were observed under ×25 magnification. The individual microvessels were counted in five different fields (center, north, west, east and south) from three hot-spots. Isolated or clusters of CD31-positive endothelial cells were considered as single countable vessels. For each tumor, the vessel density (MVD) was expressed as the mean number of vessels counted in 30 different fields (two slides, three hot-spots, five fields) per mm2.

Protein tumor extraction for VEGF and bFGF quantification. Samples of tumor were embedded and snap-frozen in a matrix gel for cryostat sectioning (Sakura Tissue Tek O.C.T. compound; Finetek, Flemmingweg, the Netherlands). The protein extraction from frozen O.C.T.-embedded tumor samples was performed as described elsewhere (5). Protein quantitative assessment was performed by a colorimetric protein assay with bicinchoninic acid (BCA) (Sigma, Saint Louis, MO, USA). bFGF and VEGF detection in replicate of protein extracts from tumor was realized with quantitative ELISA kits for human bFGF and VEGF detection (RayBio, Norcross, Canada). The results expressed in pg/ml were normalized by the total protein concentration in all samples and were expressed in nanograms of VEGF or bFGF per mg total protein.

Statistics. The statistical analyses (Stat view version 5.0; SAS Institute Inc., Cary, NC, USA) included a non-parametric Mann–Mann & Whitney *U*-test to compare the tumor volume, MVD, VEGF and bFGF concentrations between groups. Spearman's test was used to verify if parameters such as tumor growth, VEGF and bFGF concentration were correlated. Results were considered significant when $p<0.05$.

Results

Transfection of VX2 cell line with rabbit bFGF cDNA encoding vector. VX2 cell line was successfully transfected. Two clones of bFGF-transfected cells were selected: CL#1

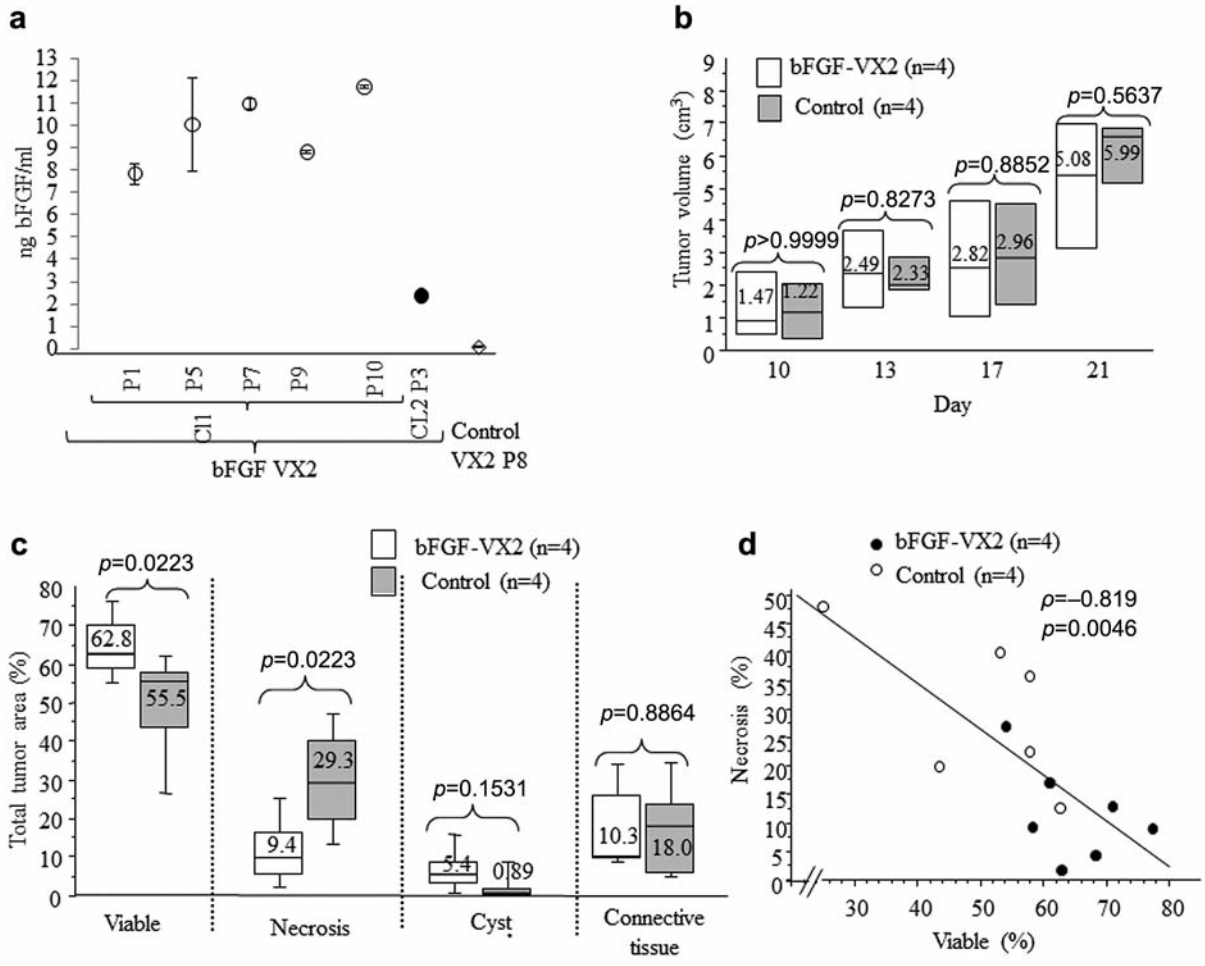

Figure 1. *a: Basic fibroblast growth factor (bFGF) concentrations in culture supernatant of transfected and control cells were measured in duplicate samples by enzyme-linked immunosorbent assay. Data represent the average of the duplicate samples values±standard deviation b: Evolution of tumor volume overtime as determined by ultrasound for bFGF-VX2 and control tumors. c: Percentage of the total tumor area represented by viable, necrotic, cystic and connective tissue. In the box plot, the distance between the whiskers represents percentiles (90% of total values), the upper and lower box boundaries represent the first and third quartiles, respectively, and the central bar indicates the median. d: Percentage of necrosis was negatively correlated with the percentage of viable tumoral tissue. CL: CIone; P: passage.*

producing 9.9±1.64 ng/ml and CL#2 producing 2.38±0.14 bFGF ng/ml. A very low level of bFGF was detected in control-VX2 cells media (0.063±0.05 ng/ml). CL#1 was selected because it was stable for *in vitro* bFGF secretion for 10 subcultures (from 7.84±0.47 at P1 to 11.74±0.04 at P10) and produced 157 times more bFGF than the control, non-transfected VX2 cell line (Figure 1a).

Tumor growth. In both groups, bFGF-VX2 and control, only four out of five transplantations led to tumor growth. The presence of tumor was monitored by ultrasound from the tenth day after implantation. No significant differences were observed between groups regarding the tumor volume measured by ultrasound at any time over the 21-day period (Figure 1b).

Histological evaluation. bFGF-VX2 transfected tumors had the highest percentage of viable tumoral tissue when compared to controls (p=0.0223; Figure 1c, 2a and c). The viable tissue was homogenously distributed in bFGF-VX2 tumors, unlike the controls for which the viable tissue was observed at the periphery, surrounding the areas of necrosis (Figure 2a and b). The level of necrosis was significantly lower in bFGF-VX2 tumor, when compared to parental tumors (p=0.0223, Mann–Whitney). A negative correlation was observed between viable and necrotic tumoral tissue (ϱ=–0.819, p=0.0046) (Figure 1d). Small areas of necrosis were homogenously distributed in the bFGF-VX2 tumors, whereas in controls large areas of necrosis were observed in the tumor core (Figure 2b and d). Necrosis involved damaged cells that lacked cohesion, had an eosinophilic

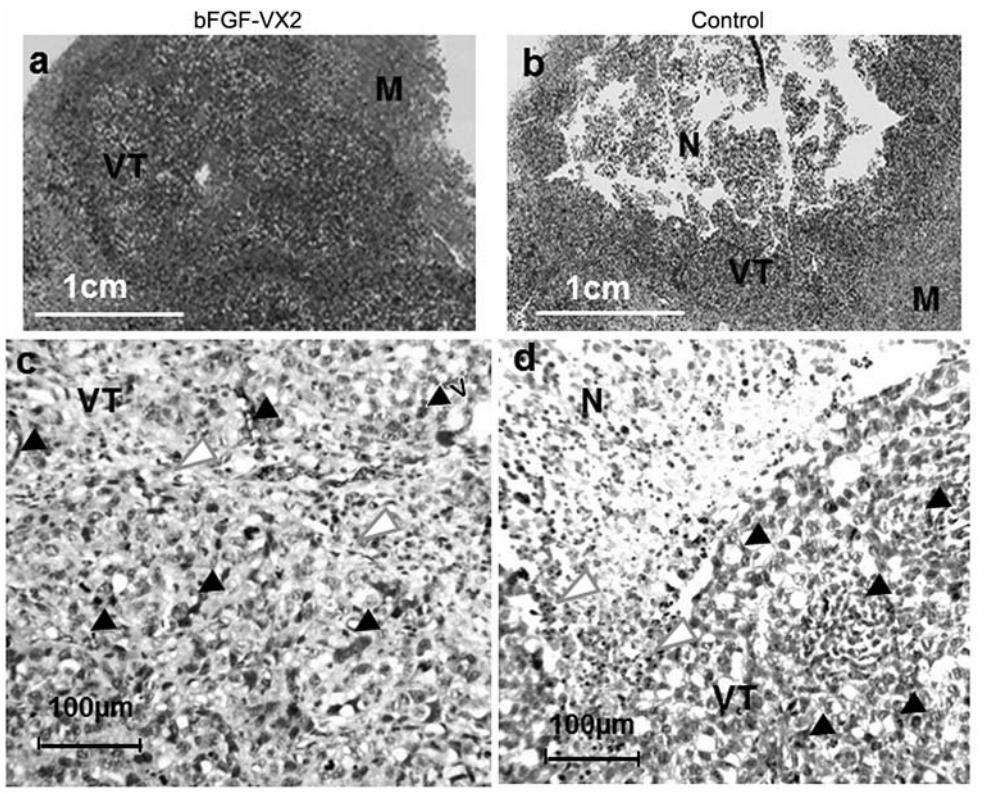

Figure 2. *Digitized images of hematoxylin-eosin-saffron-stained tumors (areas enclosed by dashed line) revealed large area of viable tumoral tissue (VT) in basic fibroblast growth factor (bFGF)-transfected VX2 tumors (a) and extensive zones of necrosis (N) in the tumor core for control-VX2 tumors (b). c, d: Vessel distribution in the CD31-stained tumors. bFGF-VX2 tumors contained vessels (black arrows) homogenously distributed in viable tissue (VT) (c). Control tumors presented vessels distributed at the tumor edges surrounding the large areas of necrosis (N) in the tumor core (d). M: Muscle.*

cytoplasm, condensation of their nuclei, and shrunken appearance (Figure 2b).

Limited area of cysts were detected and quantified for bFGF-VX2 tumors as small, round or oval shaped distributed all over the tumor. In the a control group, small areas of cysts were present in the core of the tumor, close to the necrotic area.

The percentage of connective tissue was not different between transfected and control tumors (Figure 1d). In the controls, the connective tissue was mainly distributed around the tumors, whereas in tumors from bFGF transfected cells, many fibers of connective tissue were observed crisscrossing the tumors, accompanying the vessels, and at the tumor edges, surrounding the tumoral tissue. Foci of inflammatory cells were observed in bFGF-VX2 tumors infiltrating the connective tissue. The predominant inflammatory cells were eosinophils, whereas in control tumors, mainly lymphocytes and macrophages were seen, that infiltrated the tumor edges and the periphery of necrotized areas of the tumor.

Immunohistochemical CD31 staining and MVD. In the bFGF-VX2 group, vessels were homogenously distributed all over the tumor, with regular diameters, and an aspect similar to vessels observed in control tumor (Figure 2c). In the control group, vessels were heterogeneously distributed, dense vascularization was observed at the tumor edges surrounding the central area containing many areas of necrosis (Figure 2d).

The MVD for bFGF-VX2 transfected tumors was not significantly different from that of the control group (p=0.3444, Mann–Whitney) (Figure 3c).

bFGF and VEGF concentration in tumors. bFGF concentration was significantly greater in bFGF-VX2 tumors than in controls (p=0.0062, Mann–Whitney; Figure 3a). The bFGF protein concentration in tumors was negatively, inversely correlated with the tumor volume at day 21 (ϱ=–0.927, p=0.0034).

The VEGF concentration in tumors overexpressing bFGF was significantly lower than in controls (p=0.0105, Mann–Whitney; Figure 3b) and negatively correlated with the bFGF concentration (ϱ=–0.903, p=0.0067).

Discussion

The transfection of VX2 cells with bFGF-encoding vector can produce clones expressing stable levels of bFGF.

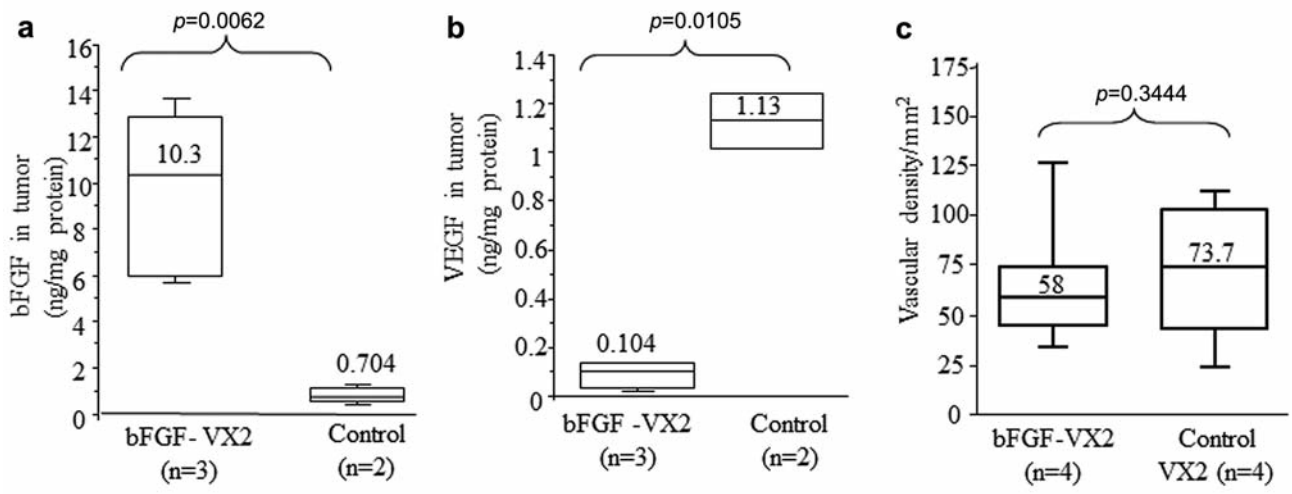

Figure 3. *Basic fibroblast growth factors (bFGF) (a) and vascular endothelial growth factor (VEGF) (b) concentrations in bFGF-transfected and control VX2 tumors as measured in duplicate samples by enzyme-linked immunosorbent assay. c: Vascular density for bFGF-transfected and control VX2 tumors was quantified on tumor slices stained with anti-CD31. In the box plot, the distance between the whiskers represents percentiles (90% of total values), the upper and lower box boundaries represent the first and third quartiles, respectively, and the central bar indicates the median.*

Implantation of these clones induced tumors more viable and three times less necrotized than non-transfected control tumors. In previous work of our group, we demonstrated that VEGF modified VX2 tumors, which became larger, more vascular and half as necrotized as controls (5).

In the present study, non-transfected control tumors at 21 days had a volume, area of necrosis and vascularization in line with those already reported in the literature (4, 10-13).

We surprisingly found that overexpression of bFGF in VX2 tumors had no effect on tumor volume. Our finding contrasts with studies demonstrating that bFGF overexpression in carcinoma cells induced tumors of greater volume and vascular density than parental cells (6, 8). In accordance with others however (14-16), bFGF expression is not consistently associated with tumor growth. It has been found that bFGF dose-dependently inhibits the growth of tumor cells *in vitro* and *in vivo* by inducing apoptosis, the death of tumor cells, or by cell-cycle arrest in G_1 (15-17). In fact, the effects of bFGF on tumor cells seem to depend on the microenvironment as it can act either as a cell growth inhibitor in the presence of growth factors from serum, or as a mitogenic factor in hormone-deprived medium (16). Under our *in vitro* conditions, the growth of bFGF-VX2 cells was not inhibited despite the presence of growth factors in culture. One can assume that *in vivo*, many different factors (*e.g.* hormones, and growth factors) could interfere with the growth of bFGF-VX2 tumors.

In our study, we found a reduction of necrosis in bFGF-VX2 tumors, which is in agreement with most data of the literature establishing an anti-apoptotic role of bFGF on tumor cells overexpressing bFGF (18).

MVD of bFGF-VX2 tumors did not differ from that of control tumors. This finding contrasts with the many reports demonstrating a direct implication of bFGF in MVD enhancement and the growth of tumors overexpressing bFGF (6) or constitutively expressing bFGF (19). Our results are in line with previous studies showing that bFGF (over)expression is not necessarily associated with MVD increase in tumors (7, 8). In breast carcinoma xenografts overexpressing bFGF, two types of vessels were observed: stromal vessels involved in providing oxygen and nutrients to the tumor cells, and tumor edge-associated vessels, corresponding to vessels in hot spots of human tumors, involved in tumor growth and expansion (7). In our model, we could suppose that bFGF promotes the development of the vessels playing rather a role of feeding vessels than of vessels involved in tumor expansion and angiogenesis. This could explain the low level of necrosis in these tumors. Secondly, a condition for bFGF to be able to augment MVD and to induce aggressive tumors is for it to be secreted into the extracellular space, as was described for fibrosarcoma (20). We can suppose that under our experimental conditions, bFGF produced by bFGF-VX2 cells may not sufficiently diffuse to act as mitogenic factor on the vessels from tumor edges, responsible for tumor growth. Probably only VEGF acts as a mitogenic factor for the vessels from tumor edges in the VX2 model since VEGF-VX2 transfected tumors exhibited an increased volume and vessel density (5). This hypothesis is sustained by the fact that bFGF tumors expressed very low levels of VEGF and therefore had a decreased MVD and volume.

Limitations and Perspective

This model requires a large number of cells to make the inoculum and therefore a series of *in vitro* culture of cells prior to implantation. The development of tumor beyond 21 days, in terms of growth, necrosis, vascular density and fibrosis remains to be clarified.

Conclusion

We successfully obtained a stable VX2 clone producing high amounts of bFGF *in vitro* and *in vivo*. Overexpression of bFGF in VX2 cells increased the percentage of viable tumoral tissue, diminished necrosis threefold, modified the architecture of the tumors but had no effect on tumor volume or MVD.

This new phenotype of VX2 tumor could offer some advantages over the classical VX2 model for evaluating anticancer therapies. Thanks to its lower level of necrosis compared to the classical model, bFGF-VX2 tumors may allow evaluation of the long-term efficacy (*i.e.* over several weeks) of chemotherapies.

References

1 Kidd JG and Rous P: A transplantable rabbit carcinoma originating in a virus-induced papilloma and containing the virus in masked or altered form. J Exp Med *71*: 813-838, 1940.

2 Es RJJv: The Rabbit VX2 Auricle Carcinoma An Animal Model for Development of New Locoregional Treatment Strategies Against Squamous Cell Carcinoma of the Head and Neck. Ph.D. thesis. University Medical Center Utrecht, Netherland: pp. 1-140, 2001.

3 Gaba RC, Emmadi R, Parvinian A and Casadaban LC: Correlation of doxorubicin delivery and tumor necrosis after drug-eluting bead transarterial chemoembolization of rabbit VX2 liver tumors. Radiology 152099, 2016 (http://dx.doi.org/10.1148/radiol.2016152099).

4 Vossen JA, Buijs M, Geschwind JF, Liapi E, Prieto Ventura V, Lee KH, Bluemke DA and Kamel IR: Diffusion-weighted and Gd-EOB-DTPA-contrast-enhanced magnetic resonance imaging for characterization of tumor necrosis in an animal model. J Comput Assist Tomogr *33*: 626-630, 2009.

5 Pascale F, Ghegediban SH, Bonneau M, Bedouet L, Namur J, Verret V, Schwartz-Cornil I, Wassef M and Laurent A: Modified model of VX2 tumor overexpressing vascular endothelial growth factor. J Vasc Interv Radiol *23*: 809-817, 2012.

6 McLeskey SW, Kurebayashi J, Honig SF, Zwiebel J, Lippman ME, Dickson RB and Kern FG: Fibroblast growth factor 4 transfection of MCF-7 cells produces cell lines that are tumorigenic and metastatic in ovariectomized or tamoxifen-treated athymic nude mice. Cancer Res *53*: 2168-2177, 1993.

7 McLeskey SW, Tobias CA, Vezza PR, Filie AC, Kern FG and Hanfelt J: Tumor growth of FGF or VEGF transfected MCF-7 breast carcinoma cells correlates with density of specific microvessels independent of the transfected angiogenic factor. Am J Pathol *153*: 1993-2006, 1998.

8 Graeven U, Rodeck U, Karpinski S, Jost M, Philippou S and Schmiegel W: Modulation of angiogenesis and tumorigenicity of human melanocytic cells by vascular endothelial growth factor and basic fibroblast growth factor. Cancer Res *61*: 7282-7290, 2001.

9 Yoshiji H, Kuriyama S, Yoshii J, Ikenaka Y, Noguchi R, Hicklin DJ, Huber J, Nakatani T, Tsujinoue H, Yanase K, Imazu H and Fukui H: Synergistic effect of basic fibroblast growth factor and vascular endothelial growth factor in murine hepatocellular carcinoma. Hepatology *35*: 834-842, 2002.

10 Verheul HM, Panigrahy D, Yuan J and D'Amato RJ: Combination oral antiangiogenic therapy with thalidomide and sulindac inhibits tumour growth in rabbits. Br J Cancer *79*: 114-118, 1999.

11 Zhang J, Wang R, Lou H, Zou Y and Zhang M: Functional computed tomographic quantification of angiogenesis in rabbit VX2 soft-tissue tumor before and after interventional therapy. J Comput Assist Tomogr *32*: 697-705, 2008.

12 Stewart EE, Chen X, Hadway J and Lee TY: Correlation between hepatic tumor blood flow and glucose utilization in a rabbit liver tumor model. Radiology *239*: 740-750, 2006.

13 Sugimoto K, Moriyasu F, Kamiyama N, Metoki R and Iijima H: Parametric imaging of contrast ultrasound for the evaluation of neovascularization in liver tumors. Hepatol Res *37*: 464-472, 2007.

14 Rubatt JM, Darcy KM, Hutson A, Bean SM, Havrilesky LJ, Grace LA, Berchuck A and Secord AA: Independent prognostic relevance of microvessel density in advanced epithelial ovarian cancer and associations between CD31, CD105, p53 status, and angiogenic marker expression: A Gynecologic Oncology Group study. Gynecol Oncol *112*: 469-474, 2009.

15 Wang H, Rubin M, Fenig E, DeBlasio A, Mendelsohn J, Yahalom J and Wieder R: Basic fibroblast growth factor causes growth arrest in MCF-7 human breast cancer cells while inducing both mitogenic and inhibitory G1 events. Cancer Res *57*: 1750-1757, 1997.

16 Fenig E, Wieder R, Paglin S, Wang H, Persaud R, Haimovitz-Friedman A, Fuks Z and Yahalom J: Basic fibroblast growth factor confers growth inhibition and mitogen-activated protein kinase activation in human breast cancer cells. Clin Cancer Res *3*: 135-142, 1997.

17 Sturla LM, Westwood G, Selby PJ, Lewis IJ and Burchill SA: Induction of cell death by basic fibroblast growth factor in Ewing's sarcoma. Cancer Res *60*: 6160-6170, 2000.

18 Li D, Wang H, Xiang JJ, Deng N, Wang PP, Kang YL, Tao J and Xu M: Monoclonal antibodies targeting basic fibroblast growth factor inhibit the growth of B16 melanoma *in vivo* and *in vitro*. Oncol Rep *24*: 457-463, 2010.

19 Zhang W, Chu YQ, Ye ZY, Zhao ZS and Tao HQ: Expression of hepatocyte growth factor and basic fibroblast growth factor as prognostic indicators in gastric cancer. Anat Rec *292*: 1114-1121, 2009.

20 Kandel J, Bossy-Wetzel E, Radvanyi F, Klagsbrun M, Folkman J and Hanahan D: Neovascularization is associated with a switch to the export of bFGF in the multistep development of fibrosarcoma. Cell *66*: 1095-1104, 1991.

Received April 12, 2016
Revised May 17, 2016
Accepted May 24, 2016